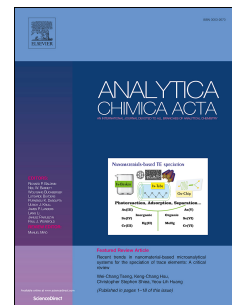


# Accepted Manuscript

Combined optical and electronic paper-nose for detection of volatile gases

Yu Chen, Rachel E. Owyueung, Sameer R. Sonkusale



PII: S0003-2670(18)30739-6

DOI: [10.1016/j.aca.2018.05.078](https://doi.org/10.1016/j.aca.2018.05.078)

Reference: ACA 236015

To appear in: *Analytica Chimica Acta*

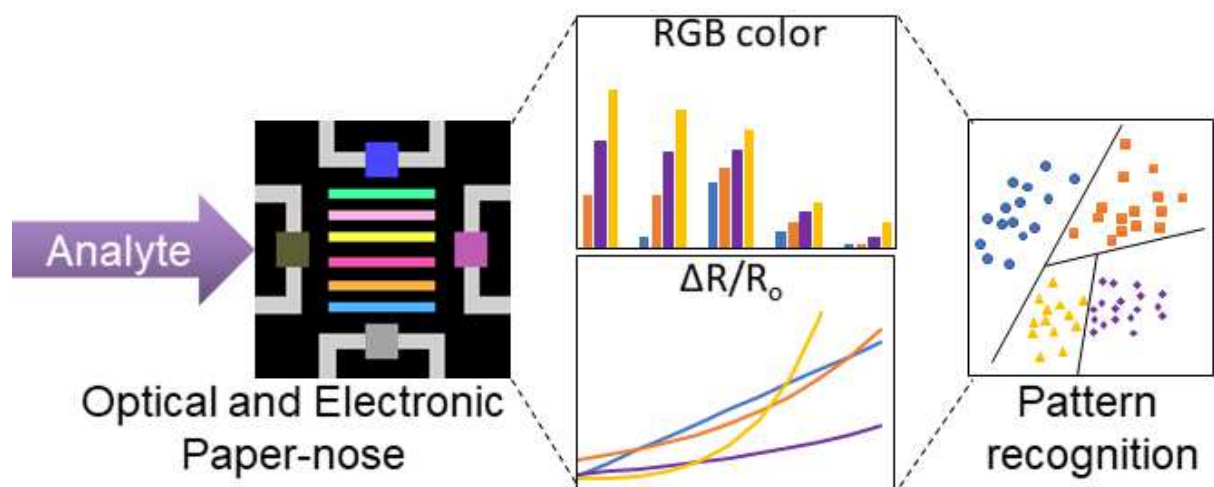
Received Date: 5 February 2018

Revised Date: 14 May 2018

Accepted Date: 31 May 2018

Please cite this article as: Y. Chen, R.E. Owyueung, S.R. Sonkusale, Combined optical and electronic paper-nose for detection of volatile gases, *Analytica Chimica Acta* (2018), doi: 10.1016/j.aca.2018.05.078.

This is a PDF file of an unedited manuscript that has been accepted for publication. As a service to our customers we are providing this early version of the manuscript. The manuscript will undergo copyediting, typesetting, and review of the resulting proof before it is published in its final form. Please note that during the production process errors may be discovered which could affect the content, and all legal disclaimers that apply to the journal pertain.



# Combined optical and electronic paper-nose for detection of volatile gases

Yu Chen<sup>a,c</sup>, Rachel E. Owyung<sup>b,c</sup> and Sameer R. Sonkusale<sup>a,c\*</sup>

<sup>a</sup>*Electrical and Computer Engineering Department, Tufts University, Medford, MA 02155, USA*

<sup>b</sup>*Chemical Engineering Department, Tufts University, Medford, MA 02155, USA*

<sup>c</sup>*Nano Lab, Advanced Technology Laboratory, Tufts University, Medford, MA 02155, USA*

## Abstract

In this work, a paper-based optoelectronic sensor (paper-nose) is presented for sensing volatile gases in air. The proposed optoelectronic sensor is a combination of both colorimetric (optical) and chemiresistive (electronic) sensor arrays in order to improve the selectivity of the paper-nose in the complex air background. The optical sensors are based on chemoresponsive dyes, namely Reichardt's dye (2,6-diphenyl-4-(2,4,6-triphenyl-1-pyridinio)phenolate), bromocresol purple, methyl red, bromothymol blue, brilliant yellow and manganese tetraphenylporphyrin (Mn-TPP). The chemiresistive sensors are based on nanomaterials, such as carbon nanotubes (CNT), PEDOT:PSS, graphite, and an ionic liquid, 1-ethyl-3-methylimidazolium bis(trifluoromethylsulfonyl)imide (EMI TFSI). Sensor is fabricated through direct handwriting of sensing materials using a pen on paper without the need of expensive cleanroom facilities. The optoelectronic sensor is tested in ambient air with different volatile gases such as methanol, ammonia, toluene, acetone and ethanol and their mixtures of varying concentrations. The detected electrical and optical responses together form a unique signature for each volatile gas and its mixture. Support-vector machine (SVM) is applied for target classification and detection. From the SVM result, it is found that better discriminative power is achieved by combining optical and electrical responses.

*Keywords:* paper-nose, paper diagnostics, optoelectronic, volatile gases, environment sensing

## 1. Introduction

Volatile organic compounds (VOCs) are ubiquitous and abundant in our environment, as they are generated both naturally by the metabolic activities of plants and animals, and anthropogenically by organic chemicals, coal and biomass burning, and the petrochemical industry. VOCs can be harmful to human health when present in the air in excessive amounts, both for short-term [1] and long-term exposures [2]. Given the effect of chronic toxicity, it is necessary to monitor their concentrations in the environment. So far, the detection and discrimination of various VOCs can be realized by using various gas sensing techniques, including optical (e.g. absorption spectroscopy) [3], electrical (electronic nose) [4], gas chromatography (GC) [5], acoustic [6], and photo-ionization techniques [7,8].

Commercially, VOC sensors are combined with other features such as temperature and humidity monitoring, but still lack the ability to distinguish between many of the individual VOCs detected [8,9]. Optical sensor arrays with chemo-responsive dyes have been proposed as a portable, highly sensitive, cost-effective method for VOCs detection and classification. Janzen et al. [10] built a colorimetric sensor array containing metalloporphyrins, pH indicator dyes and solvatochromic dyes and tested the response for 24 VOCs including a range of aldehydes, carboxylic acids, alcohols, ketones, and aromatic amines, to name a few. It is observed that these colorimetric sensor arrays can generate a unique color pattern for each VOC. The successful detection and discrimination of VOCs using colorimetric sensing arrays offers a reliable method for real-time monitoring of VOCs. Another comparable gas sensing technique is dubbed the electronic nose. Electronic nose refers to chemiresistive sensor arrays built with sensing elements (e.g. nanomaterials) that change resistance upon chemical exposure [11]. The functionality of the

electronic nose is realized through integrating chemiresistive sensor arrays with different sensing materials onto one platform to increase the range of gases it can reliably sense. In Moon's work [12], chemiresistive sensor arrays based on SnO<sub>2</sub>, WO<sub>3</sub> and In<sub>2</sub>O<sub>3</sub> were realized to sense VOCs found in breath, such as H<sub>2</sub>S, NH<sub>3</sub>, and NO, to name a few. Gas detection is possible through monitoring of the electrical properties (e.g. resistance) of each chemiresistive sensor to obtain an ensemble collective response. The amount of resistance change is used to analyze the presence and amount of the specific volatile gas. Current commercial VOC sensors are often based on PIDs, electrochemical sensors, or metal oxide (MOx) sensors [8,9]. While MOx sensors have been commercialized, research still continues to move towards facile fabrication and single MOx layer selectivity [13,14]. Recently, carbon materials, including carbon nanotubes and graphene, and conductive polymers, [15] such as polypyrrole [16], polyaniline [17,18], and poly(3,4-ethylene-dioxythiophene) [19] have been successfully demonstrated for gas sensing in research settings. These carbon-based materials provide wide range of choices for sensing elements in making the next generation of chemiresistive sensor arrays. In recent studies, functionalizing nanomaterials (e.g. nanowire, nanoparticles) with various molecular groups to form novel gas sensing elements has gradually become popular due to the improved stability and sensitivity [20–23]. In Peng et al. [24], gold nanoparticles were capped with different thiol groups (e.g. dodecanethiol, butanethiol) and used to build sensor arrays for breath testing with ppb level sensitivity.

The optical or electrical gas sensors discussed above and in most of the prior arts are built on some commonly used substrates, including silicon and silica [12,25]. For people to perform their own air quality monitoring in their environment, there is a need to develop a new type of gas sensors, which are easier to fabricate using an environmentally friendly process and are cost

effective. Moreover, these sensors should be compact, portable and easy to use, and must provide a rapid and accurate response. Most of the currently available gas sensing techniques, however accurate, require expensive equipment such as a light spectrometer, and some expertise in operating it. One approach to lower the cost is to employ cheaper substrates for making the sensor itself. Variety of materials, such as plastic, polymer and paper, can be employed as a substitute of traditional sensor substrates [26,27]. Of these, common cellulosic paper substrates have caught much attention due to its ubiquity, cost and eco-friendliness [28] and is also the substrate of choice in this paper.

So far, paper-based sensors have been used in many applications including biomedical diagnostics (e.g. glucose sensing, blood testing) [29,30], chemical sensing (e.g. metal ion detection) [31], and mechanical sensing (e.g. strain sensor) [32]. Paper's hydrophilic nature allows for a wide variety of materials to be functionalized directly on paper without treatment. For example, drop casting conductive ink enables easy construction of electrical sensing elements on paper [33]. Single-sensing-element-based chemiresistive sensors have been built on paper substrate for gas sensing [34]. One successful example of a paper based gas chemiresistive sensor is realized by using a CNT pencil to directly draw CNTs on the interdigitated gold electrodes pre-deposited on the paper substrate [35]. This sensor has been successfully used for ammonia sensing. However, the progress on paper-based nose (or paper-nose) is still limited to handful of volatile gases with continued research aiming to improve its range, sensitivity, and selectivity [36].

In this work, we have functionalized a paper substrate with a variety of chemoresponsive dyes and conductive nanomaterials as chemiresistors to form an optoelectronic sensor arrays for gas sensing. The chemoresponsive dyes were selected to create a mix of pH indicators,

metalloporphyrins, and solvatochromic dyes, thus providing means of detecting different types of chemical properties of a given VOC for improved sensor diversity [10,28,37]. Similarly, the chemiresistors were chosen with a similar goal in mind. Here, we use multiple carbon allotropes, ionic liquids, and conductive polymers to promote sensor diversity [19,35,38]. The materials chosen are shown to be sensitive, but their individual responses are not robust in by themselves. However, we show that the ensemble response from the combined chemiresistive and colorimetric sensors improves the overall selectivity and the robustness of the paper-nose sensor platform.

Several common volatile gases (e.g. methanol, ammonia, toluene), as well as the mixture of different gases, have been tested with this optoelectronic paper-nose platform. A machine learning method using support vector machines (SVM) has been applied to classify the responses to different gas analytes with accuracy better than individual electronic or optical responses alone.

## 2. Experimental

### 2.1 Preparation of sensing elements

The fabrication of the paper-based optoelectronic sensor arrays is realized through direct handwriting of sensing materials directly on paper similar to the approach discussed previously [33]. The details are described as follows:

All chemicals were purchased from Sigma Aldrich unless stated otherwise. Six chemoresponsive dyes were chosen to include pH indicators, metalloporphyrins, and solvatochromic dyes for sensing diversity, namely 2,6-Diphenyl-4-(2,4,6-triphenyl-1-pyridinio)phenolate (Reichardt's dye), bromocresol purple, methyl red, bromothymol blue, brilliant yellow, manganese tetraphenylporphrin (Mn-TPP). The dyes were mixed in ethanol (99.5%) to create a 0.5 % (w/v)

solution that was vortexed until fully dissolved. Their chemical structures can be found in supplementary Figure S1. PEDOT:PSS, EMI TFSI, graphite, and CNTs make up the chemiresistive electronic response. EMI TFSI (EMD Millipore) was mixed with pentaerythritol tetraacrylate in a 15 wt% solution to adhere it to the paper substrate. An 8B pencil serves as the source of graphite. PEDOT:PSS and CNTs were used as received. PEDOT:PSS and EMI TFSI structures can be found in supplementary Figure S2. SEM images of the chemiresistive materials are shown in supplementary Figure S3 to illustrate the morphology of the deposited materials on chromatography paper after sensing. The results show agreement with reported images of these materials deposited on paper, indicating that the nanomaterials are not detrimentally modified from their use in sensing these VOCs [39–41]. Figure 1 shows the Raman spectra obtained for each of the chemiresistive materials. Three prominent peaks often observed for carbon nanomaterials are the G' band ( $\sim 2700 \text{ cm}^{-1}$ ), G band ( $\sim 1580 \text{ cm}^{-1}$ ), and the D band ( $\sim 1350 \text{ cm}^{-1}$ ), which can be observed for the CNT and graphite samples in Figure 1 (a) and (b), respectively. The CNT and graphite sample display the characteristic D, G, and G' bands as reported in literature [42]. The broadness and asymmetrical shape of the G' band indicate a graphite sample. The sum of interactions between the stacked graphene layers leads to a wider peak. The G to D band relative intensity is used to measure the quality of the carbon nanomaterial, as the D band arises due to edge effects of the graphene structure. The relative intensities of the G to D band between the CNT and graphite spectra indicate that the CNT sample is more ordered, as expected. The ionic liquid sample, EMI TFSI, shows a narrow, yet high intensity peak around  $740 \text{ cm}^{-1}$ , as shown in Figure 2 (c). This is due to the strong C-F interaction of the ionic liquid [43]. The PEDOT:PSS spectra, shown in Figure 2 (d), displays ring stretching peaks close to  $1570 \text{ cm}^{-1}$ ,  $1440 \text{ cm}^{-1}$ , and  $1360 \text{ cm}^{-1}$ , similar to values reported previously [44]. Since we

\* Corresponding author. Tel.: +1- 617-627-5113. E-mail address: sameer@ece.tufts.edu

observe similar Raman spectra as reported in literature for each of our chemiresistive materials, we can say that the modification of the chromatography paper with these materials did not impact the chemical properties and therefore the sensing properties of these chemiresistive materials. All Raman spectra were obtained using a laser wavelength of 532 nm (DXR from ThermoScientific).

### *2.2 Patterning of the paper substrate*

The sensor layout is pre-designed in Solidworks (Version 2016) and then transferred onto the Whatman cellulose chromatography paper (3001-861 Grade 1 CHR) through wax printing via Xerox ColorQube 8580 printer, as illustrated in Figure 2 (a). The wax-printed paper is placed on a hot plate at 85°C to allow uniform penetration of wax through the whole thickness of the paper substrate (0.18 mm). The sensor layout can be seen in supplementary Figure S4. Briefly, each nanomaterial patch is 5 mm x 5 mm and each optical patch is 1.5 mm x 15 mm. The total sensor size is 37.5 mm x 37.5 mm.

### *2.3 Functionalization of the patterned paper substrate*

The sensing materials are directly written onto the designated areas by refillable pen or using cotton swab dipped in them. The electrical contacts are made by writing AG-510 silver conductive ink from Applied Ink Solutions onto the contact areas (Figure 2 (a)).

### *2.4 Encapsulation of the as-fabricated paper-nose*

The as-functionalized sensor is encapsulated in a sealed custom-designed acrylic chamber to allow simultaneous electrical and optical measurements. The custom-designed acrylic chamber has inlet and outlet, which allows the gas to flow through the chamber. The chamber is used for test and validation but could be optional when used in real-life applications.

### *2.5 Test setup and data acquisition*

Figure 2 (b) shows the schematic of test set up. The targeted gas analytes, including methanol, ammonia, toluene, acetone, and ethanol (ASC reagent grade, Sigma Aldrich), are prepared through bubbling air into each liquid analyte using a 4 mL bubbler (Sigma Aldrich). A gas mixing system is created using two acrylic gas flow meters to control the flow rates of the targeted gas with flow rate control of  $7.87\text{e-}7 - 7.87\text{e-}6 \text{ m}^3/\text{s}$  (0.1-1 Standard Cubic feet per hour (SCFH)) and a control of  $7.87\text{e-}6 - 7.87\text{e-}5 \text{ m}^3/\text{s}$  (1-10 SCFH) of pure air. The targeted gas and air of different flow rates are mixed to obtain different analyte concentration (7.5%, 15%, 50%) by tuning the flow rates of pure air and targeted analyte gas that are mixed. Due to the differences in gas volatility and the dependence of the volatility on temperature and pressure, estimations for concentration vary by analyte. For example, Ammonia concentrations were around 55, 110, and 365 ppm for 7.5%, 15%, and 50%, respectively. Toluene, which has a much higher density, was around 308, 617, and 2055 ppm for 7.5%, 15%, and 50%. These are sensitivity levels seen for as-assembled sensors which can be improved easily through improved fabrication process and improved color sensitivity of commercial cameras on the phone. The gas mixture is then passed through the sensing chamber depicted in Figure 2 (a). To measure the sensor responses at each gas concentration, the targeted gas flows through the chamber continuously for 20 min to get a stable response. For recovery between measurements, 100% pure air (no contribution from the VOC flow meter) is flown through the chamber for 30 min. Humidity levels of the test gas were found to be <10%, the lowest reading, using a Pros Kit NT-312 temperature and humidity monitor. Effects of humidity on electronic noses has been discussed previously [8,45]. One can add a relative humidity correction factor to all the measured output. Correction factors can be acquired by fitting the sensor response under different humidity conditions [46]. The gas mixtures of combined target analyte compounds MAT (methanol,

\* Corresponding author. Tel.: +1- 617-627-5113. E-mail address: sameer@ece.tufts.edu

acetone and toluene) and MNE (methanol, ammonia and ethanol) are prepared by first mixing the pure methanol, acetone and toluene solution (or methanol, ammonia and ethanol solution) at the volume ratio of 1:1:1. Then, the solution mixture (either MAT or MNE) is filled into a bubbler; finally, air is bubbled into each solution mixture to get the desired gas mixture.

In the experiment, the optical responses are collected by taking the images of the optical sensor arrays using a USB microscope camera from Plugable Technologies (USB2-Micro-200X). The camera is fixed above the sensing chamber and maintains a relatively uniform illumination for all the images. The electrical responses can be obtained through a LabVIEW program (Version 2016, National Instruments, US) controlled DAQ card (National Instruments USB-6008). For characterization purpose, the conductance of each chemiresistor in the electrical sensor arrays is measured using a digital multimeter (Fluke 115 True RMS Multimeter). To obtain quantitative values of optical signals, the red (R), green (G), and blue (B) channel intensities, the color channels in the RGB additive color model, of each chemoresponsive dye are extracted from the images of optical sensor arrays. This work uses the RGB color model to store the unique color information as three integer values, all between 0 and 255 (the range a single 8-bit byte can offer), with 0 indicating no color contribution from that channel, and 255 representing the brightest contribution from that channel. Each shown R, G, B intensity value is the average of a region in each color bar in the image. The electrical responses are presented by the amount of conductance change (%) of each chemiresistor.

Support-vector machine (SVM) classifier with linear Kernel function [47] is used to classify the sensor responses to seven different gases and mixtures using MATLAB (Mathworks US, Version 2016). This supervised classification model uses leave p-out cross-validation (LpO CV) statistics, where nine observations are used as the validation set and the remaining eight

observations are used as the training set. The unbalanced dataset is dealt by repeating training and validating the model n choose k (9+8, 8) times where each training cycle has different set of observations. All the repeated experiments are done using 17 different devices. In all the experiments, one device is used to test one gas analyte with three repeated measurements, so that the accuracy of obtained signal pattern for one specific analyte can be guaranteed and the interacting signal from other analytes can be eliminated.

### **3. Results and discussion**

#### *3.1 Sensing volatile gases*

The optoelectronic paper-nose platform is used to monitor five volatile gases, namely methanol, ammonia, toluene, acetone and ethanol. Figure 3 illustrates the sensors' optical responses to different targeted gases. It is observed that the color change of these optical sensor arrays varied with different gases, resulting in different color patterns. This is because the selected chemo-responsive dyes have varying sensitivity towards different gases. Based on this property, a unique color pattern is formed for each gas, which acts as the optical signature for the specific gas. For example, Mn-TPP was more sensitive to ammonia, toluene, and acetone compared to methanol, while Reichardt's dye showed color change for all different gases, with a significant shift after exposure to acetone. For each gas analyte, a gradual color change of optical dyes is observed from low concentration to high concentration, indicating the capability of optical sensor arrays to distinguish gases of different concentrations. For example, MR shows a slow shift from red to yellow in the presence of ammonia.

In Figure 4, the responses of electrical sensor arrays to targeted gases of different concentrations (methanol, ammonia, toluene, acetone and ethanol) is summarized. It is found that the electrical sensor arrays have different sensitivities towards different gases. For example, we

observe that electrical sensors are highly sensitive to ammonia, while having low sensitivity to toluene. In all experiments, the full devices made were tested in triplicate for each measurement. Compared with optical responses, it is more difficult to distinguish targeted gases using electrical sensor arrays alone due to the similarity in the resulting response pattern. If one could generate a multi-dimensional vector for each gas that combines the RGB optical responses and the conductance change from the electrical responses, this vector will have a distinguishable signature to enable distinction between different gases. The distinction is measured using a suitable distance metric between these vectors using an SVM machine learning algorithm discussed below.

### *3.2 Sensing volatile gases mixtures*

The optoelectronic sensors in the paper-nose demonstrated the capability to sense and distinguish gases. We also demonstrate the paper-nose's capability of sensing complex gas mixtures. To perform such evaluation, two gas mixtures, MAT (methanol, acetone and toluene) and MNE (methanol, ammonia and ethanol) are prepared for testing. These two gas mixtures are prepared as discussed above and are flown through the gas chamber with varying concentrations using the same apparatus as before. The optical and electrical responses of these sensor arrays in the paper-nose are recorded, as shown in Figure 5(a-c). Color changes are observed for the bromocresol purple and Reichardt's dye for the MAT mixture, and conductance changes are observed in the PEDOT:PSS and ionic liquid as concentration of the mixture increases. In comparison, the MNE mixture shows color changes across the entire optical sensor array, and we see changes in all four chemiresistive elements in higher magnitude versus the MAT mixture. Figure 6 represents the amount of change of sensor's optical and electrical responses during the gas sensing process normalized over gray scale. Briefly, the optical signal from each sensing dye

is decomposed into R,G,B signal, the values of R,G,B signal of the specific dye during gas sensing were compared with its original R,G,B values, and the percentage of change of these R,G,B values were calculated as the inputs to generate a gray scale (0-100%) distribution of the change of response from each sensing element during gas sensing. Same with the electrical sensing elements, for which the changes of resistance were recorded and a gray scale (0-100%) distribution is plotted together with the gray-scale change of optical signals. Thus, the darker shadings indicate a larger change in sensor response due to exposure. Each column represents the response pattern to a specific gas analyte. By combining the optical and electrical responses, a combined gray-scale map provides a visually more discriminative signature for each gas. For instance, the optical responses of ethanol and MAT are highly similar, but the electrical responses clearly show the difference; for acetone and MAT, the electrical responses are almost identical while the optical responses are different. Similar observation can be found when comparing the sensor responses to toluene and MAT. All these observations demonstrate an enhancement in paper-nose's discriminative capability towards different gas analytes, compared with the situation of using electrical sensors or optical sensors alone.

### *3.3 Classification of paper-nose responses*

SVM training and classification is performed using the leave-p out cross-validation approach discussed in section 2.5. For SVM classification, eight measurements for each class of gas are selected and trained by SVM classifier. The obtained model for each class is used to test the untrained observed responses (9 points). Classification is performed on three categories of data: combination of optical and electrical responses, only optical responses and only electrical responses. The classification results for three categories of data are shown in Table 1. It is found that even though the electrical sensor arrays respond to all gas analytes with different

sensitivities, electrical responses alone are not sufficient to distinguish different gases, given the significant number of mismatch points and much higher error rate. Optical sensor arrays alone performed much better than electrical sensors in gas discrimination, with significant lower number of mismatch points and error rate. By combining both optical and electrical responses, lower error rate and perfect classification is achieved, which shows the improvement of paper-nose's discriminative power. The optical and electrical responses together form a complete set of sensor responses to each gas analyte. More importantly, all the sensing is performed in complex air background suggesting real life applicability of paper-nose in detection of volatile gases in air.

#### **4. Conclusion**

In this work, a paper-based optoelectronic sensor platform aka paper-nose with optical and electrical sensor arrays is presented for sensing volatile gases and its mixtures in air. The collective response from optical and electrical sensor arrays forms a unique signature for each gas analyte and their mixtures. Sensitivity to wide range of gases is possible due to the diversity of sensing materials used such as nanomaterials as chemiresistors and chemoresponsive dyes. The individual responses are cross-reactive (not selective) and selectivity is achieved by capturing the ensemble response from all the sensing components, both electrical and optical, which collectively demonstrate unique signature to an analyte. The target range of gases and selectivity to them can be improved even further by expanding this library of sensing elements. The platform is built on paper substrate using direct writing of sensing materials on paper without the need for expensive facilities and thus reduces the cost for fabrication and improves the possibility of widespread adoption. The application of this gas sensor is not limited to the selected gases described here, but can be easily extended to other volatile organic compounds.

#### **Acknowledgement**

REO's effort was partially supported by NSF IGERT grant (DGE-1144591). The authors would like to thank Dr. Hojatollah Rezaei Nejad for help with figures.

ACCEPTED MANUSCRIPT

## References

- [1] L. Mølhave, B. Bach, O.F. Pedersen, Human reactions to low concentrations of volatile organic compounds, *Environ. Int.* 12 (1986) 167–175. doi:10.1016/0160-4120(86)90027-9.
- [2] J. Kesselmeier, M. Staudt, Biogenic Volatile Organic Compounds (VOC): An Overview on Emission, Physiology and Ecology, *J. Atmos. Chem.* 33 (1999) 23–88.  
<https://link.springer.com/content/pdf/10.1023/A:1006127516791.pdf> (accessed November 6, 2017).
- [3] D.W. Van Der Weide, J. Murakowski, F. Keilmann, Gas-absorption spectroscopy with electronic terahertz techniques, *IEEE Trans. Microw. Theory Tech.* (2000). doi:10.1109/22.841967.
- [4] J.A. Deshmukh Sharvari, Bandyopadhyay Rajib, Bhattacharyya Nabarun, Pandeya R.A., Application of electronic nose for industrial odors and gaseous emissions measurement and monitoring – An overview, *Talanta*. 144 (2015) 329–340. doi:10.1016/J.TALANTA.2015.06.050.
- [5] J. Kopka, Gas Chromatography Mass Spectrometry, in: *Plant Metabolomics*, Springer-Verlag, Berlin/Heidelberg, 2006: pp. 3–20. doi:10.1007/3-540-29782-0\_1.
- [6] W. Xuan, M. He, N. Meng, X. He, W. Wang, J. Chen, T. Shi, T. Hasan, Z. Xu, Y. Xu, J.K. Luo, Fast Response and High Sensitivity ZnO/glass Surface Acoustic Wave Humidity Sensors Using Graphene Oxide Sensing Layer, *Sci. Rep.* 4 (2015) 7206. doi:10.1038/srep07206.
- [7] J.G.W. Price, D.C. Fenimore, P.G. Simmonds, A. Zlatkis, Design and operation of a photoionization detector for gas chromatography, *Anal. Chem.* 40 (1968) 541–547. doi:10.1021/ac60259a013.
- [8] F. Röck, N. Barsan, U. Weimar, Electronic Nose: Current Status and Future Trends, (2007). doi:10.1021/cr068121q.
- [9] B. Szulczyński, J. Gębicki, Currently Commercially Available Chemical Sensors Employed for Detection of Volatile Organic Compounds in Outdoor and Indoor Air, *Environments*. 4 (2017) 21. doi:10.3390/environments4010021.
- [10] M.C. Janzen, J.B. Ponder, D.P. Bailey, C.K. Ingison, K.S. Suslick, Colorimetric Sensor Arrays for Volatile Organic Compounds, *Anal. Chem.* 78 (2006) 3591–3600. doi:10.1021/ac052111s.
- [11] D.K. Aswal, S.K. Gupta, Science and technology of chemiresistor gas sensors, Nova Science Publishers, 2007.  
<https://books.google.com/books?hl=en&lr=&id=bMRubqYylHgC&oi=fnd&pg=PR7&dq=D.+K.+Aswal+and+S.+K.+Gupta,+Science+and+Technology+of+Chemiresistor+Gas+S>

ensors&ots=QgOLyJNOQ2&sig=FeEmJuhEreSZA#v=onepage&q=D.  
K. Aswal and S. K. Gupta%2C Science and Technology of Chemiresistor Gas  
Sensors&f=false (accessed November 6, 2017).

- [12] H.G. Moon, Y. Jung, S.D. Han, Y.-S. Shim, B. Shin, T. Lee, J.-S. Kim, S. Lee, S.C. Jun, H.-H. Park, C. Kim, C.-Y. Kang, Chemiresistive Electronic Nose toward Detection of Biomarkers in Exhaled Breath, *ACS Appl. Mater. Interfaces.* 8 (2016) 20969–20976. doi:10.1021/acsami.6b03256.
- [13] W. Yang, P. Wan, M. Jia, J. Hu, Y. Guan, L. Feng, A novel electronic nose based on porous In<sub>2</sub>O<sub>3</sub> microtubes sensor array for the discrimination of VOCs, *Biosens. Bioelectron.* 64 (2014) 547–553. doi:10.1016/j.bios.2014.09.081.
- [14] S. Hwang, H. Kwon, S. Chhajed, J. Won Byon, J. Min Baik, J. Im, S. Ho Oh, H. Won Jang, S. Jin Yoon, J. Kyu Kim, A near single crystalline TiO<sub>2</sub> nanohelix array: enhanced gas sensing performance and its application as a monolithically integrated electronic nose, *Analyst.* 138 (2013) 443–450. doi:10.1039/C2AN35932D.
- [15] B.D. Lampson, Y.J. Han, A. Khalilian, J.K. Greene, D.C. Degenhardt, J.O. Hallstrom, Development of a portable electronic nose for detection of pests and plant damage, *Comput. Electron. Agric.* 108 (2014) 87–94. doi:10.1016/j.compag.2014.07.002.
- [16] P.-G. Su, Y.-T. Peng, Fabrication of a room-temperature H<sub>2</sub>S gas sensor based on PPY/WO<sub>3</sub> nanocomposite films by in-situ photopolymerization, *Sensors Actuators B Chem.* 193 (2014) 637–643. doi:10.1016/j.snb.2013.12.027.
- [17] V. Talwar, O. Singh, R.C. Singh, ZnO assisted polyaniline nanofibers and its application as ammonia gas sensor, *Sensors Actuators B Chem.* 191 (2014) 276–282. doi:10.1016/j.snb.2013.09.106.
- [18] J. Qi, X. Xinxin, X. Liu, K.T. Lau, Fabrication of textile based conductometric polyaniline gas sensor, *Sensors Actuators B. Chem.* 202 (2014) 732–740. doi:10.1016/j.snb.2014.05.138.
- [19] Y. Yang, S. Li, W. Yang, W. Yuan, J. Xu, Y. Jiang, In Situ Polymerization Deposition of Porous Conducting Polymer on Reduced Graphene Oxide for Gas Sensor, *ACS Appl. Mater. Interfaces.* 6 (2014) 13807–13814. doi:10.1021/am5032456.
- [20] E. Espid, F. Taghipour, Development of highly sensitive ZnO/In<sub>2</sub>O<sub>3</sub> composite gas sensor activated by UV-LED, *Sensors Actuators B Chem.* 241 (2017) 828–839. doi:10.1016/j.snb.2016.10.129.
- [21] D. Zhang, A. Liu, H. Chang, B. Xia, Room-temperature high-performance acetone gas sensor based on hydrothermal synthesized SnO<sub>2</sub>-reduced graphene oxide hybrid composite, *RSC Adv.* 5 (2015) 3016–3022. doi:10.1039/C4RA10942B.
- [22] X. Yang, V. Salles, Y.V. Kaneti, M. Liu, M. Maillard, C. Journet, X. Jiang, A. Brioude, Fabrication of highly sensitive gas sensor based on Au functionalized WO<sub>3</sub> composite nanofibers by electrospinning, *Sensors Actuators B Chem.* 220 (2015) 1112–1119.

doi:10.1016/j.snb.2015.05.121.

- [23] J. Liu, T. Wang, B. Wang, P. Sun, Q. Yang, X. Liang, H. Song, G. Lu, Highly sensitive and low detection limit of ethanol gas sensor based on hollow ZnO/SnO<sub>2</sub> spheres composite material, Sensors Actuators B. 245 (2017) 551–559.  
doi:10.1016/j.snb.2017.01.148.
- [24] G. Peng, U. Tisch, O. Adams, M. Hakim, N. Shehada, Y.Y. Broza, S. Billan, R. Abdah-Bortnyak, A. Kuten, H. Haick, Diagnosing lung cancer in exhaled breath using gold nanoparticles, Nat. Nanotechnol. 4 (2009) 669–673. doi:10.1038/nnano.2009.235.
- [25] K.S. Suslick, An Optoelectronic Nose:“Seeing” Smells by Means of Colorimetric Sensor Arrays, MRS Bull. 29 (2004) 720–725. doi:10.1557/mrs2004.209.
- [26] Y.S. Kim, Microheater-integrated single gas sensor array chip fabricated on flexible polyimide substrate, Sensors Actuators B Chem. 114 (2006) 410–417.  
doi:10.1016/j.snb.2005.06.016.
- [27] F. Zee, J.W. Judy, Micromachined polymer-based chemical gas sensor array, Sensors Actuators B Chem. 72 (2001) 120–128. doi:10.1016/S0925-4005(00)00638-9.
- [28] Y. Chen, Y. Zilberman, P. Mostafalu, S.R. Sonkusale, Paper based platform for colorimetric sensing of dissolved NH<sub>3</sub> and CO<sub>2</sub>, Biosens. Bioelectron. 67 (2015) 477–484.  
doi:10.1016/j.bios.2014.09.010.
- [29] T. Songjaroen, W. Dungchai, O. Chailapakul, C.S. Henry, W. Laiwattanapaisal, Blood separation on microfluidic paper-based analytical devices, Lab Chip. 12 (2012) 3392.  
doi:10.1039/c2lc21299d.
- [30] H. Liu, R.M. Crooks, Paper-Based Electrochemical Sensing Platform with Integral Battery and Electrochromic Read-Out, Anal. Chem. 84 (2012) 2528–2532.  
doi:10.1021/ac203457h.
- [31] Z. Nie, C.A. Nijhuis, J. Gong, X. Chen, A. Kumachev, A.W. Martinez, M. Narovlyansky, G.M. Whitesides, Electrochemical sensing in paper-based microfluidic devices, Lab Chip. 10 (2010) 477–483. doi:10.1039/B917150A.
- [32] H. Gullapalli, V.S.M. Vemuru, A. Kumar, A. Botello-Mendez, R. Vajtai, M. Terrones, S. Nagarajaiah, P.M. Ajayan, Flexible Piezoelectric ZnO-Paper Nanocomposite Strain Sensor, Small. 6 (2010) 1641–1646. doi:10.1002/smll.201000254.
- [33] A. Russo, B.Y. Ahn, J.J. Adams, E.B. Duoss, J.T. Bernhard, J.A. Lewis, Pen-on-Paper Flexible Electronics, Adv. Mater. 23 (2011) 3426–3430. doi:10.1002/adma.201101328.
- [34] K.A. Mirica, J.M. Azzarelli, J.G. Weis, J.M. Schnorr, T.M. Swager, Rapid prototyping of carbon-based chemiresistive gas sensors on paper, Proc. Natl. Acad. Sci. 110 (2013) E3265–E3270. doi:10.1073/pnas.1307251110.
- [35] K.A. Mirica, J.G. Weis, J.M. Schnorr, B. Esser, T.M. Swager, Mechanical Drawing of Gas Sensors on Paper, Angew. Chemie Int. Ed. 51 (2012) 10740–10745.

doi:10.1002/anie.201206069.

- [36] A. Nilghaz, L. Guan, W. Tan, W. Shen, Advances of Paper-Based Microfluidics for Diagnostics—The Original Motivation and Current Status, *ACS Sensors.* 1 (2016) 1382–1393. doi:10.1021/acssensors.6b00578.
- [37] S.H. Lim, L. Feng, J.W. Kemling, C.J. Musto, K.S. Suslick, An optoelectronic nose for the detection of toxic gases., *Nat. Chem.* 1 (2009) 562–7. doi:10.1038/nchem.360.
- [38] M.-J. Kim, E.-S. Kang, D.-W. Park, B.-S. Shim, S.-E. Shim, Ionic Liquid/Styrene-Acrylonitrile Copolymer Nanofibers as Chemiresistor for Alcohol Vapours, *Bull. Korean Chem. Soc.* 33 (2012) 2867–2872. doi:10.5012/bkcs.2012.33.9.2867.
- [39] Z. Lin, T. Le, X. Song, Y. Yao, Z. Li, K. Moon, M.M. Tentzeris, C. Wong, Preparation of Water-Based Carbon Nanotube Inks and Application in the Inkjet Printing of Carbon Nanotube Gas Sensors, *J. Electron. Packag.* 135 (2013) 11001. doi:10.1115/1.4023758.
- [40] J. Zhang, Z. Li, C. Zhang, B. Feng, Z. Zhou, Y. Bai, H. Liu, Graphite-Coated Paper as Substrate for High Sensitivity Analysis in Ambient Surface-Assisted Laser Desorption/Ionization Mass Spectrometry, *Anal. Chem.* 84 (2012) 3296–3301. doi:10.1021/ac300002g.
- [41] Y. Gao, D.J. Hassett, S. Choi, Rapid Characterization of Bacterial Electrogenicity Using a Single-Sheet Paper-Based Electrofluidic Array, *Front. Bioeng. Biotechnol.* 5 (2017) 44. doi:10.3389/fbioe.2017.00044.
- [42] M.S. Dresselhaus, G. Dresselhaus, R. Saito, A. Jorio, Raman spectroscopy of carbon nanotubes, *Phys. Rep.* 409 (2005) 47–99. doi:10.1016/j.physrep.2004.10.006.
- [43] N.R. Dhumal, K. Noack, J. Kiefer, H.J. Kim, Molecular Structure and Interactions in the Ionic Liquid 1-Ethyl-3-methylimidazolium Bis(Trifluoromethylsulfonyl)imide, *J. Phys. Chem. A.* 118 (2014) 2547–2557. doi:10.1021/jp502124y.
- [44] M. Stavytska-Barba, A.M. Kelley, Surface-Enhanced Raman Study of the Interaction of PEDOT:PSS with Plasmonically Active Nanoparticles, *J. Phys. Chem. C.* 114 (2010) 6822–6830. doi:10.1021/jp100135x.
- [45] D.R. Kauffman, A. Star, Carbon Nanotube Gas and Vapor Sensors, *Angew. Chemie Int. Ed.* 47 (2008) 6550–6570. doi:10.1002/anie.200704488.
- [46] W. Tsujita, A. Yoshino, H. Ishida, T. Moriizumi, Gas sensor network for air-pollution monitoring, *Sensors Actuators B Chem.* 110 (2005) 304–311. doi:10.1016/J.SNB.2005.02.008.
- [47] C. Cortes, V. Vapnik, Support-vector networks, *Mach. Learn.* 20 (1995) 273–297. doi:10.1007/BF00994018.

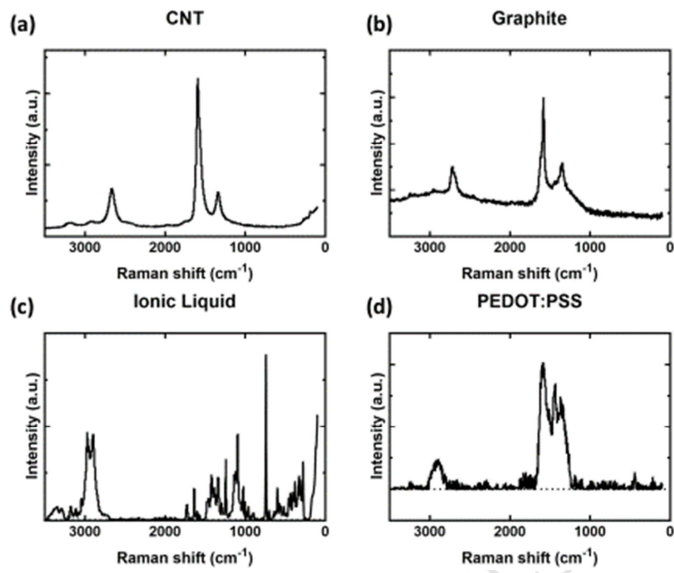
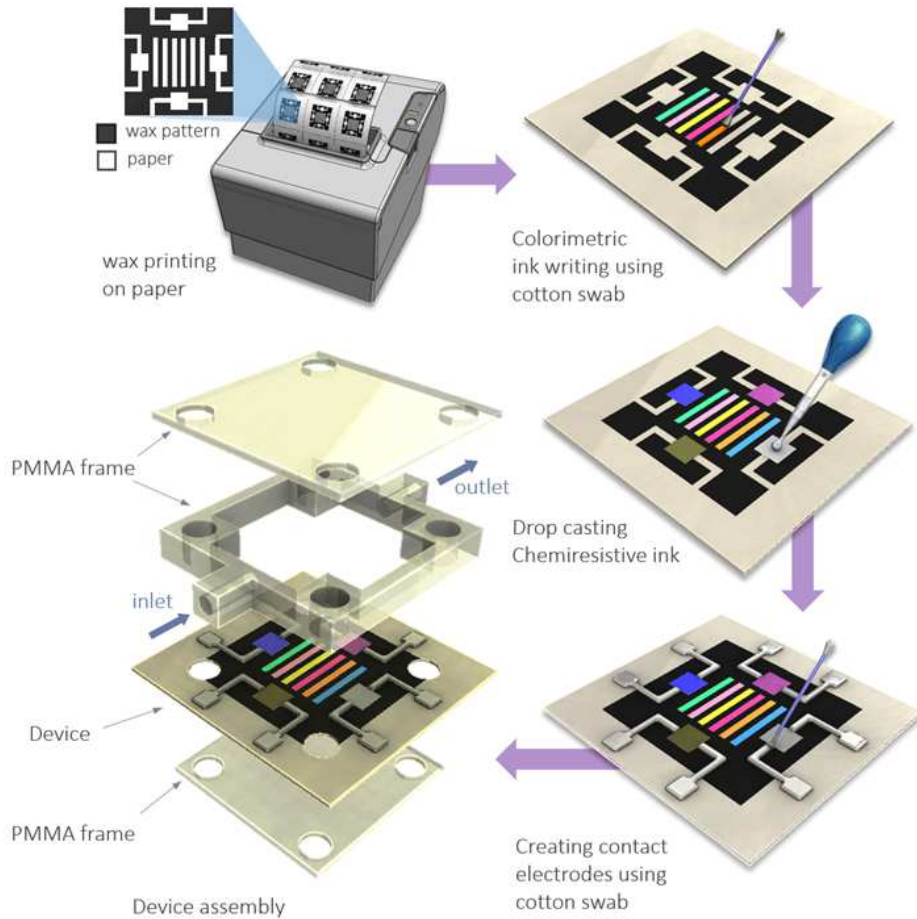
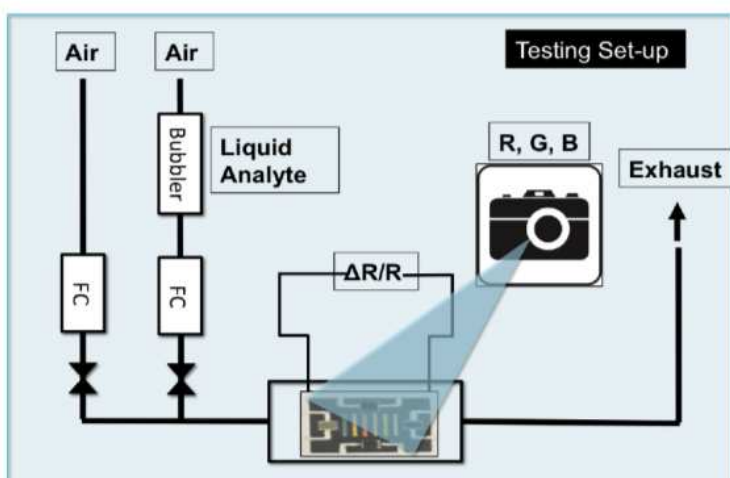


**Figure 1:** Raman spectra of a) CNTs b) graphite c) ionic liquid and d) PEDOT:PSS as deposited on paper.

a)



b)



c)

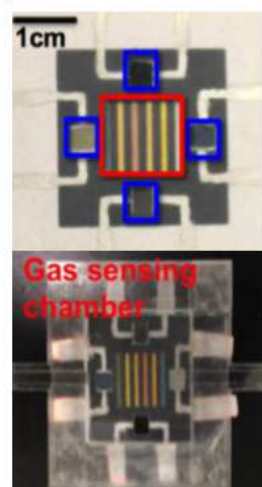


**Figure 2:** Fabrication of paper based optoelectronic sensors: (a) Patterning and functionalization: the pattern is wax printed onto chromatography paper and the optical sensors are written as stripes. Chemiresistive sensors are dropcasted onto their respective squares and electrical contacts are made for the chemiresistive sensors. The device is packaged in a custom PMMA chamber with an inlet and outlet for gas flow. (b) Test setup: gas analytes are generated by bubbling air into each liquid analyte and the flow rate of the target analyte is tuned via two flow controllers (FC) from pure air and from VOC gas. The signal readout is realized by recording the electrical resistance of chemiresistive sensors ( $\Delta R/R$ ) and taking images of optical sensors (to gather R,G,B information). (c) Full device: the paper-nose is sealed in a custom-built acrylic chamber.

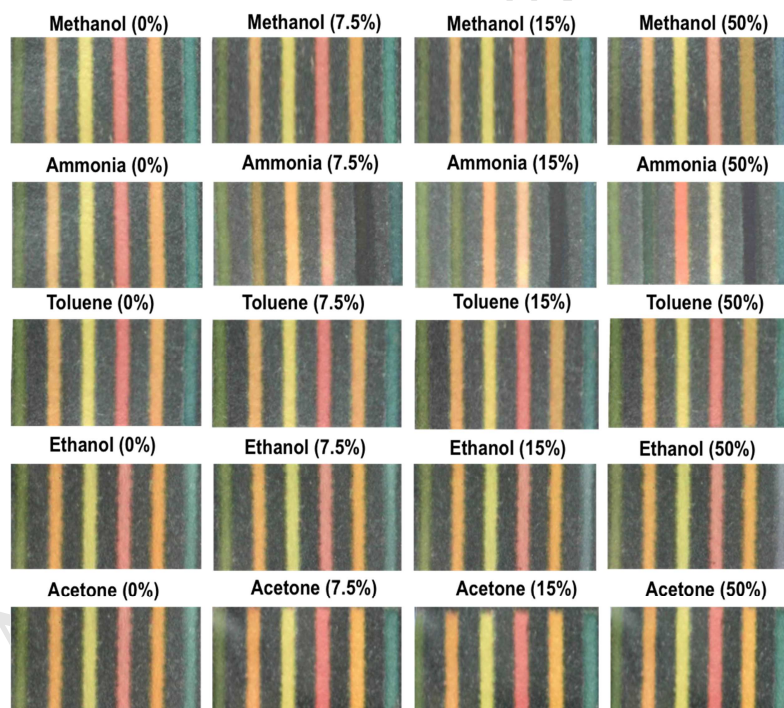


**Figure 3:** Optical responses of the optical sensing stripes of the paper-nose to 5 different gas analytes, namely methanol, ammonia, toluene, ethanol and acetone, at 3 different concentrations. Images taken by a USB camera.

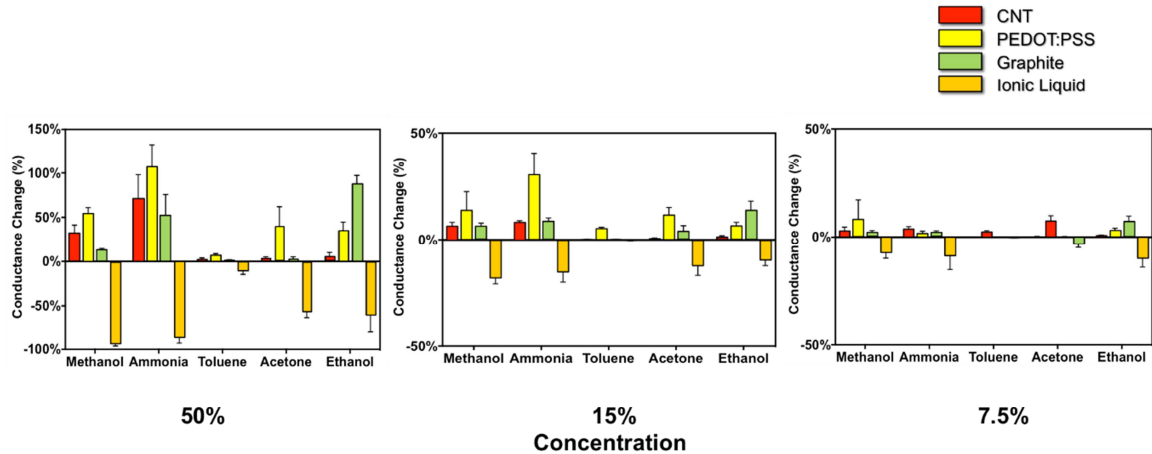


**Figure 4:** Electrical responses of the four electrical chemiresistive sensing elements of the paper-nose platform to 5 different gas analytes, namely methanol, ammonia, toluene, ethanol, and acetone, at 3 different concentrations.

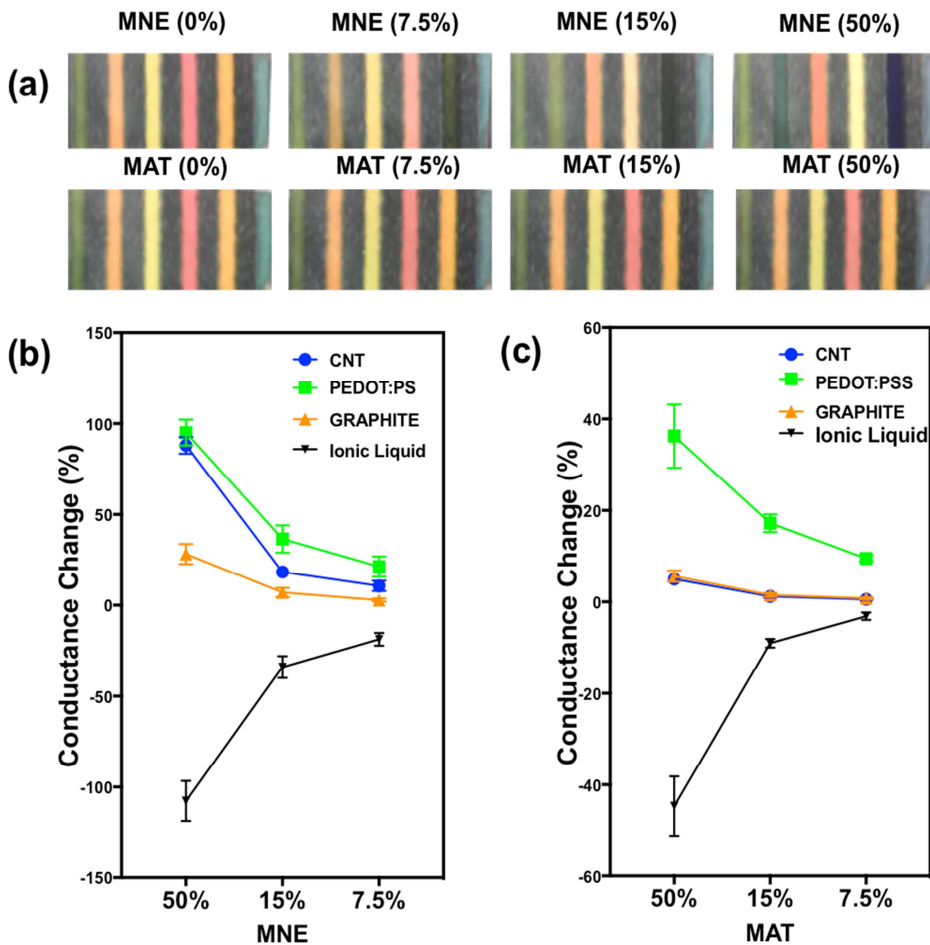


**Figure 5:** Optical and electrical responses of paper-nose platform to 2 different gas mixtures, namely MNE (methanol, ammonia, ethanol) and MAT (methanol, acetone, toluene); (a) color images of optical sensor arrays to MNE and MAT at 3 different concentrations; (b) electrical responses of electrical sensor arrays to MNE; (c) electrical responses of electrical sensor arrays to MAT.

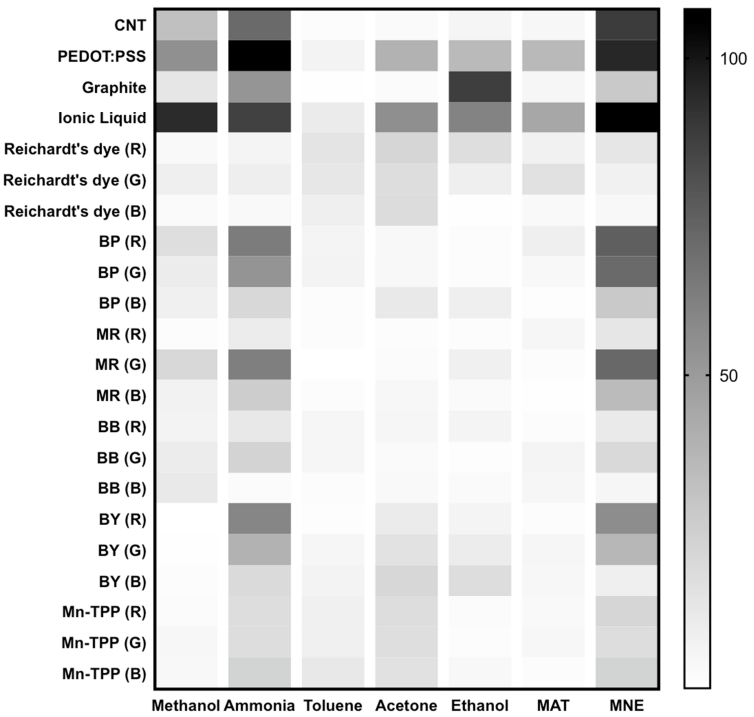


**Figure 6:** Overall responses of optoelectronic sensor arrays towards different gases and gas mixtures. The gray scale represents the absolute amount of change of each sensing element in percentage form (%). BP=bromocresol purple, MR=methyl red, BB=bromothymol blue, BY=brilliant yellow, Mn-TPP= Manganese tetraphenylporphorin.

**Table 1:** Support-vector machine (SVM) classification of paper-nose responses. There are three categories of classification: classification based on the combination of optical and electrical responses (O+E); classification of optical responses only; classification of electrical responses only.

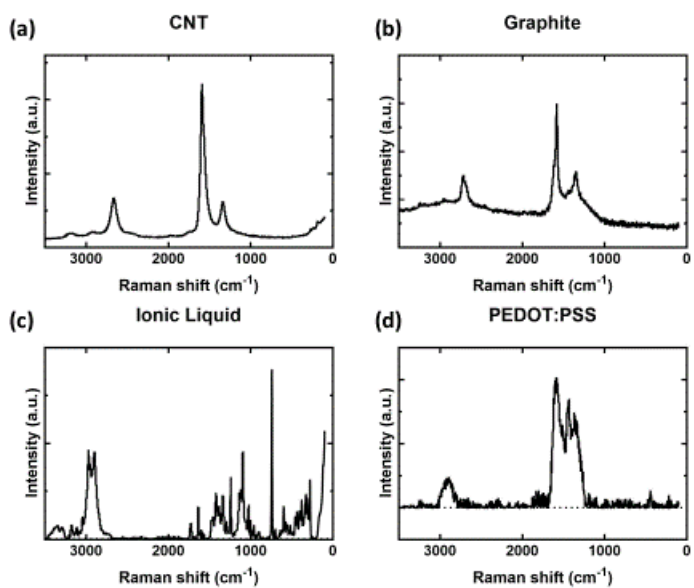
Data set	Number of accurately classified points								Error Rate
	Methanol	Ammonia	Toluene	Acetone	Ethanol	MAT	MNE		
O+E	9/9	9/9	9/9	9/9	9/9	9/9	9/9	9/9	0%
Optical	9/9	9/9	9/9	8/9	9/9	9/9	9/9	9/9	1.58%
Electrical	9/9	3/9	9/9	9/9	9/9	9/9	5/9	15.87%	

## ACCEPTED MANUSCRIPT

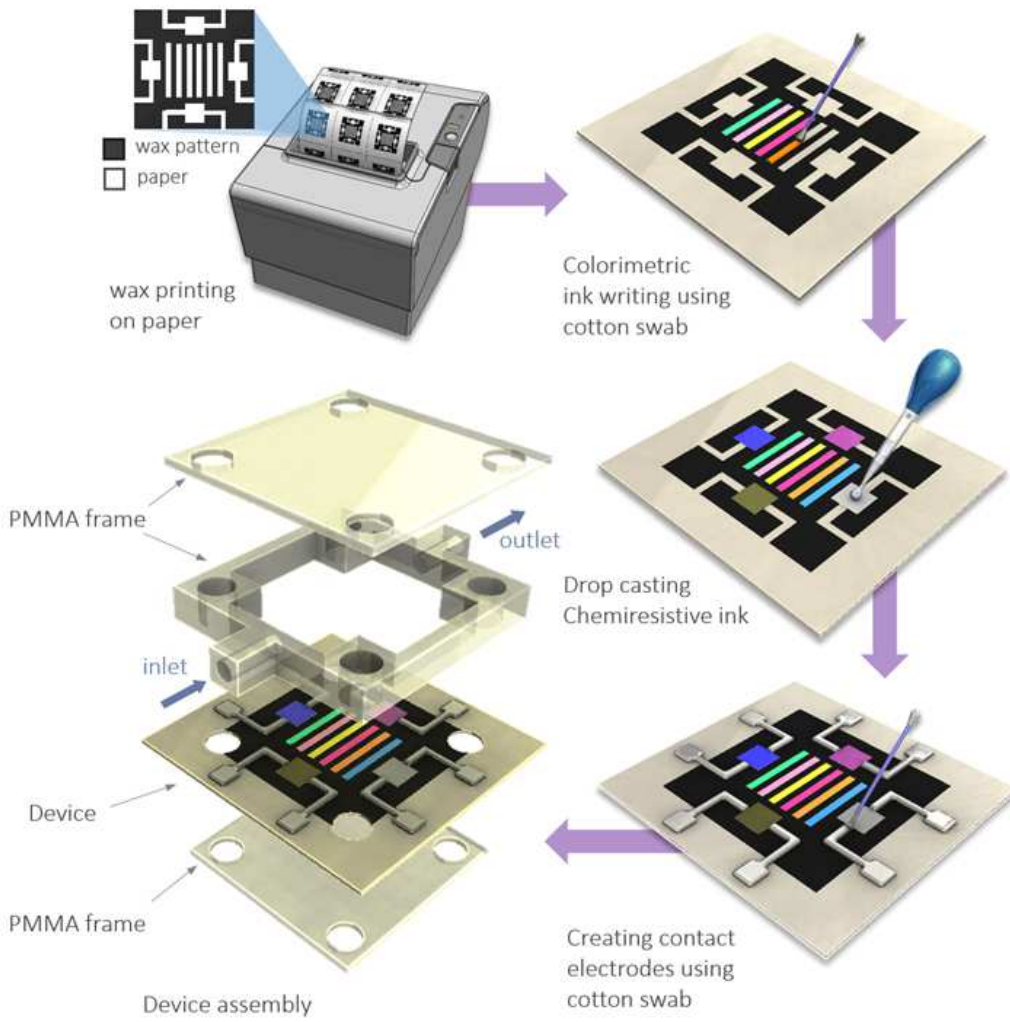
Number of accurately classified points								Error Rate
Data set	Methanol	Ammonia	Toluene	Acetone	Ethanol	MAT	MNE	
O+E	9/9	9/9	9/9	9/9	9/9	9/9	9/9	0%
Optical	9/9	9/9	9/9	8/9	9/9	9/9	9/9	1.58%
Electrical	9/9	3/9	9/9	9/9	9/9	9/9	5/9	15.87%

**Table 1:** Support-vector machine (SVM) classification of paper-nose responses. There are three categories of classification: classification based on the combination of optical and electrical responses (O+E); classification of optical responses only; classification of electrical responses only.

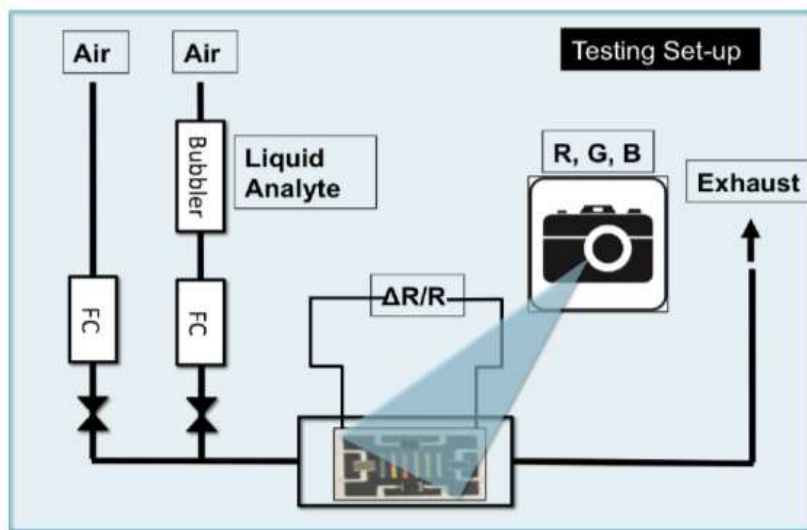
Number of accurately classified points								Error Rate
Data set	Methanol	Ammonia	Toluene	Acetone	Ethanol	MAT	MNE	
O+E	9/9	9/9	9/9	9/9	9/9	9/9	9/9	0%
Optical	9/9	9/9	9/9	8/9	9/9	9/9	9/9	1.58%
Electrical	9/9	3/9	9/9	9/9	9/9	9/9	5/9	15.87%



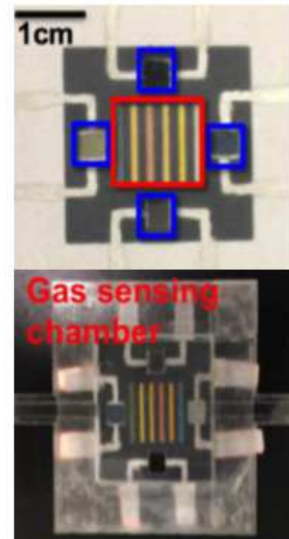
a)

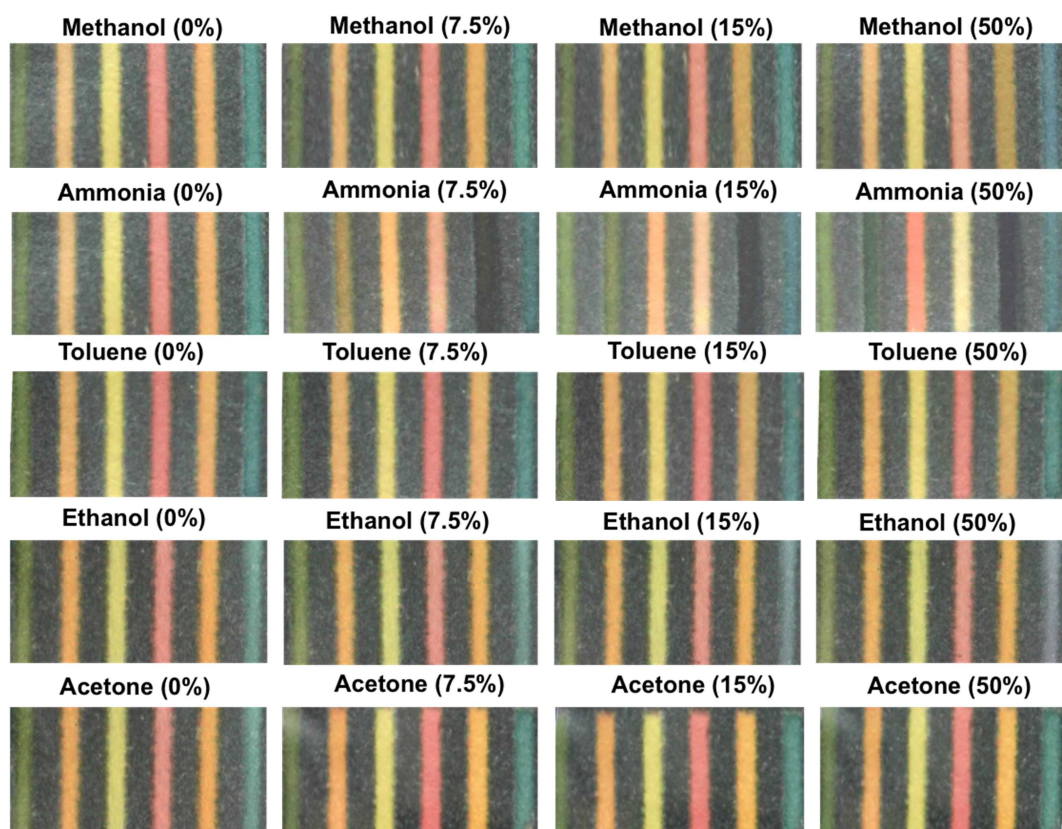


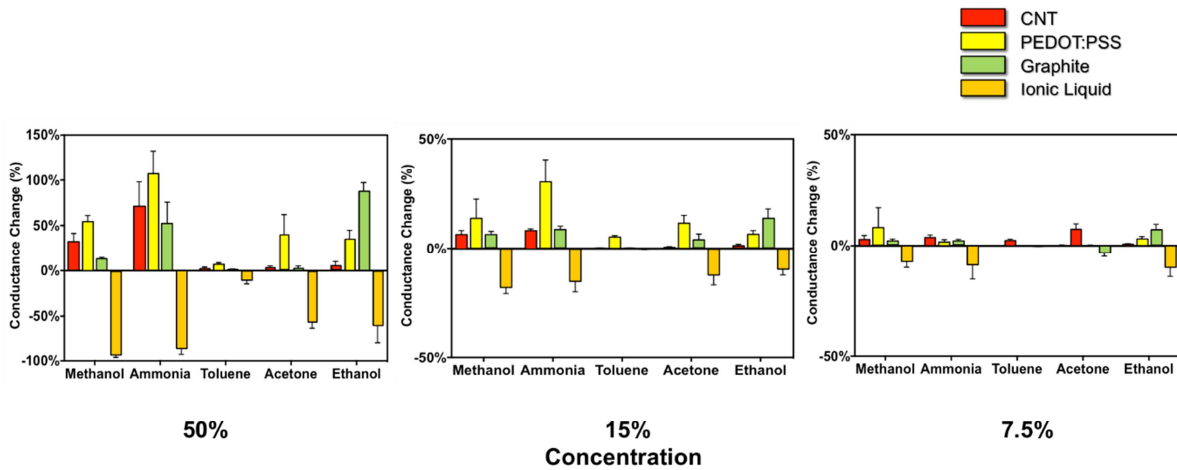
b)

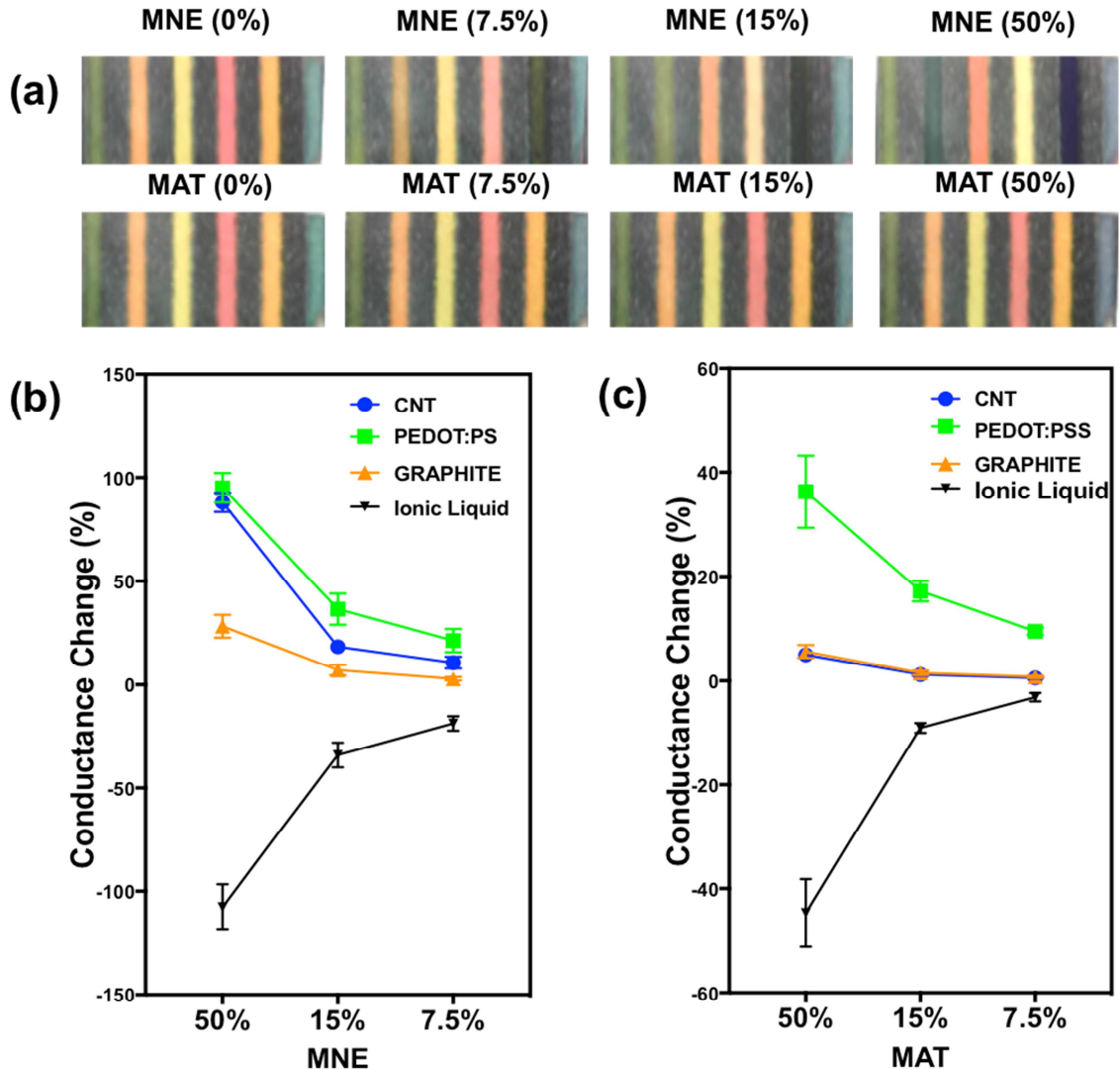


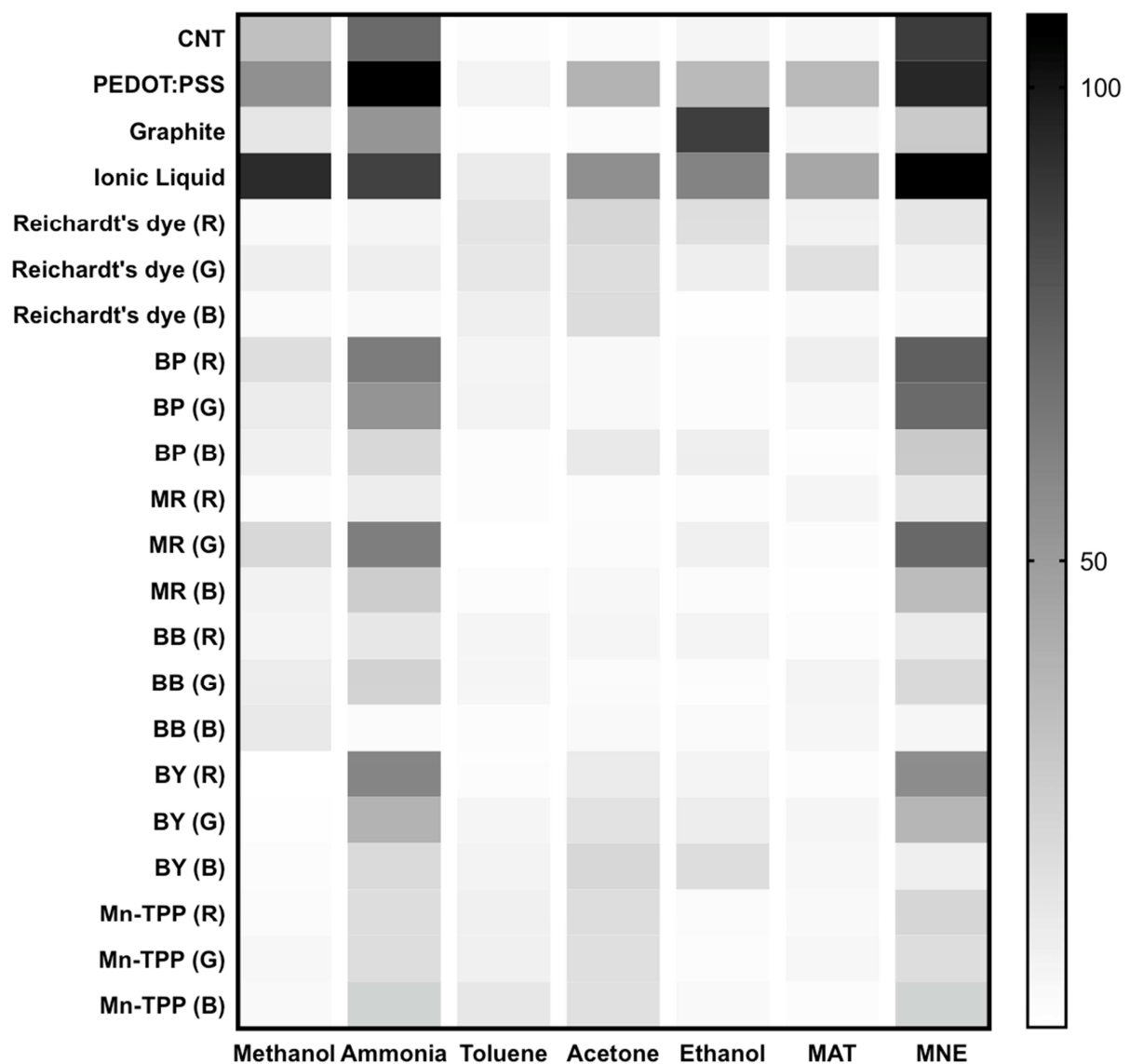
c)











## Highlights

- A paper-based optoelectronic sensor (paper-nose) with combined colorimetric (optical) and chemiresistive (electrical) sensor arrays is proposed
- The paper-nose platform is demonstrated for detection of volatile gases and complex mixtures in ambient air
- Support-vector machine classification illustrates error-free detection by use of this dual platform